PAPER

Check for updates

Surface modification of aqueous miscible organic layered double hydroxides (AMO-LDHs)†

Chunping Chen, Jean-Charles Buffet [ID] and Dermot O'Hare [ID] *

Silane modification of layered double hydroxides (LDHs) plays an important role in controlling the surface hydrophobicity and improving the compatibility of LDHs dispersed in non-polar materials. However, the surface modification of conventional LDHs in hydrous conditions typically results in aggregated particle morphologies, low surface areas and accessible pore volumes. In this study, well dispersed and high surface area silane grafted AMO-Zn_2MgAl-CO_3 LDH were prepared using the silane coupling agents (triethoxyvinylsilane (TEVS), triethoxyoctylsilane (TEOS) and (3-glycidyloxypropyl)trimethoxysilane (TMGPS)) in anhydrous acetone. Solution ^1H NMR spectroscopy was initially used to study the rate and extent of silane reactivity with AMO-Zn_2MgAl-CO_3 LDH. Powder XRD, TEM, N_2 BET specific surface area and total pore volume measurements showed that the structure and morphology of silane-treated AMO-Zn_2MgAl-CO_3 LDHs remained largely unchanged. Solid state ^{13}C CP-MAS, ^{27}Al DP-MAS and ^{29}Si CP-MAS NMR spectroscopy indicates that the silanes have been successfully grafted onto the surface of the LDH. In addition to maintaining their structure, morphology, high surface area and total pore volume, these surface-functionalised LDHs are now more hydrophobic, displaying a saturation water vapour uptake (<4 wt%) that is *ca.* 60% lower than the untreated AMO-LDH.

Introduction

Layered double hydroxides (LDHs) comprise a large family of anion exchangeable layered solids, they may be represented by the general formula $[M^{z+}_{1-x}M'^{y+}_x(OH)_2](X^{n-})_{a/n} \cdot bH_2O$, wherein M and M′ are metal cations, most commonly $z = 2$ (*e.g.* Mg^{2+}); $y = 3$ (*e.g.* Al^{3+}), $0 < x < 1$, $0 < b < 5$, giving $a = z(1 - x) + xy - 2$; X^{n-} is a charge compensating anionic moiety either organic, inorganic or biological.[1–3] Owing to their excellent anion exchangeability and good biocompatibility, LDHs have been widely used in wastewater treatment and biomolecular delivery.[4–6] The possibility of a high aspect 2D structure with a controllable layer thickness gives LDHs a promising application in gas and moisture barrier coatings on flexible polymeric films.[7–10] With the advantages of composition flexibility, homogeneous distribution of the two or more metal cations within the layers and the tunability of the number and strength of basic/acidic sites, LDHs have received considerable interest as catalysts or precursors to mixed metal oxide catalysts.[11–15]

Recently, LDHs have attracted increasing attention as a new generation of inorganic additives in polymers.[16–22] LDHs were reported to be an effective thermal and UV stabiliser in poly (vinyl chloride) (PVC). Since LDHs are intrinsically basic, they can act as acid scavenger or radical trap; both features are key factors for the thermal and UV stabilisation of PVC.[22] Dispersions of LDHs in polymers also impart excellent flame retardancy and smoke suppression properties. During combustion, LDHs undergo endothermic decomposition, absorbing heat and releasing water and CO_2 in the case of a carbonate LDHs. This LDHs facilitate absorption of heat and the formation of an expanded carbonaceous coating or char on the polymer.[17] LDHs may be intercalated with functional anions such as borate, phosphate, leading to new generations of LDHs based flame retardant materials with enhanced performance and environmentally-friendly (halogen free) character.[23–26] However, LDHs are inherently hydrophilic materials that can display very rapid moisture uptake leading to a material with a very high moisture content. This seriously affects storage, transport and the compounding of LDHs with non-polar polymers (LDHs can release the surface bound water resulting in bubble formation).

To facilitate formation of effective LDH-organic composites, a number of strategies have been previously explored to obtain LDHs containing less water and possessing hydrophobic surface character. Intercalation or surface adsorption of anionic surfactants such as sulfonates, carboxylates, phosphates and sulphates.[27–29] The interaction between these surfactants and the LDHs is mainly *via* electrostatic interactions

and hydrogen bonding. Silane modification is another promising strategy, forming chemical bonding *via* reaction of a silane with the hydroxyl groups on LDHs surface. Silanes may contain one or more functional groups enabling chemical linkages with various polymers improving their compatibility. In 2005, Park *et al.* reported that dodecylsulfate intercalated LDHs can be surface modified with silane in the presence of a cationic surfactant (*N*-cetyl-*N,N,N*-trimethylammonium bromide).[30] The formation of covalent bonding was demonstrated using solid-state ^{29}Si DP-MAS NMR spectroscopy. Wypych *et al.* studied the surface modification of LDH single sheets with (3-aminopropyl)triethoxysilane (TEAPS) in toluene.[31] However, the synthetic method required at least two steps. Subsequently, Qi *et al.* investigated a series of synthetic methods including induced hydrolysis, surfactant assisted *in situ* coprecipitation, calcination-reconstruction in Na_2CO_3 solution with direct silylation.[32–36] They found that in an aqueous environment, the silylation process is induced by hydrolysis and condensation of TEAPS on LDH surface even without any surfactant, whilst the direct silylation reaction cannot occur between the LDHs and TEAPS. The condensation reaction can only takes place between the adsorbed TEAPS and LDHs under thermal treatment. Recently, Guo *et al.* found that an LDH can be directly silylated with phenyltriethoxysilane upon reflux in toluene for 12 h.[37] However, the direct observation of the reaction between a silane and an LDH has not yet been reported. The silylation of LDHs under anhydrous conditions is still at an early stage, the challenge is to maintain particle properties such as morphology, surface area and porosity after silane modification.

In this work, we present the silane modification of Aqueous Miscible Organic Solvent Treated (AMOST) $[Zn_{0.47}Mg_{0.24}Al_{0.25}(OH)_2](CO_3)_{0.125}$ (AMO-Zn$_2$MgAl-CO$_3$ LDH) under anhydrous conditions. Three silane coupling agents, triethoxyvinylsilane (TEVS), triethoxyoctylsilane (TEOS), and (3-glycidyloxypropyl) trimethoxysilane (TMGPS) were used in this study. *In situ* solution ^{1}H NMR spectroscopy was used to monitor the rate and extent of reaction by observing the soluble products produced during the reaction between silanes and AMO-Zn$_2$MgAl-CO$_3$ LDH. The silane-modified LDH products were characterised by X-ray powder diffraction (XRD), solid-state ^{13}C CP-MAS, ^{27}Al DP-MAS and ^{29}Si CP-MAS nuclear magnetic resonance (NMR) spectroscopy, thermogravimetric analysis (TGA), transmission electron microscopy (TEM), N$_2$ Brauner–Emmett–Teller (BET) specific surface measurements and Barrett–Joyner–Halenda (BJH) total pore volume measurements. The hydrophobicity of the modified LDHs was investigated by monitoring the rate and quantity of water vapour adsorption at a range of relative humidities.

Results and discussion

The synthesis of $[Zn_{0.47}Mg_{0.24}Al_{0.25}(OH)_2](CO_3)_{0.125}\cdot0.06$ $(H_2O)\cdot0.03$(ethanol), AMO-Zn$_2$MgAl-CO$_3$ LDH, was performed in two steps. Firstly, Zn$_2$MgAl-CO$_3$ was prepared using conven-

tional co-precipitation at pH 10 followed by ageing for 16 h. Then, AMO solvent treatment was performed by dispersion of the aqueous wet solid in ethanol for 4 h. The XRD, TGA, and N$_2$ BET data for AMO-Zn$_2$MgAl-CO$_3$ LDH are shown in Fig. S4a, S7a and S9a† respectively. The chemical composition of the AMO-Zn$_2$MgAl-CO$_3$ LDH was determined by TGA, ICP and CHN combustion microanalysis. As reported previously, AMO-LDHs have enhanced surface areas and particle dispersion compared to conventionally prepared materials.[38–40] The TEM image of AMO-Zn$_2$MgAl-CO$_3$ LDH shows well dispersed LDH platelets with primary particle sizes in the range 10–250 nm (Fig. 7a). AMO-LDHs exhibit very high-water vapour uptake responses. Fig. 1 shows the time dependence of the water vapour adsorption of AMO-Zn$_2$MgAl-CO$_3$ LDH under different relative humidities at 20 °C. In a RH60 relative humidity environment, AMO-Zn$_2$MgAl-CO$_3$ LDH can adsorb up to 10 wt% water. The total water vapour uptake capacity increases with increasing relative humidity, reaching maximum of 21 wt% moisture uptake in an environment with a relative humidity of RH99. Rapid water vapour uptake is a major impediment to the usage of AMO-LDHs in moisture sensitive applications and in the applications requiring the compounding of LDHs with hydrophobic, non-polar polymers to prepare LDH-polymer nanocomposites. Hence, a silane treatment approach was developed using anhydrous conditions in order to modify the hydrophobicity of the AMO-LDH surfaces.

The AMO-LDHs were initially thermally treated to remove any surface-bound and co-intercalated water located in the interlayer galleries (maximising the available surface hydroxyl concentration). Under anhydrous conditions, the alkoxy groups of the triethoxy- or trimethoxysilanes should react with chemically accessible surface hydroxyl groups on the LDH *via* direct condensation as shown schematically in Fig. 2(a), forming new Si–O–M bonds (M = Mg, Zn, Al) to the LDH
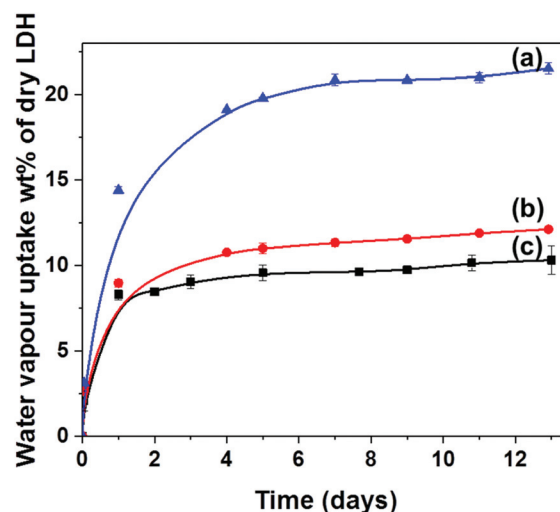

Fig. 1 Time dependence of water vapour uptake of AMO-Zn$_2$MgAl-CO$_3$ LDH in different humidity atmospheres (a) RH99, (b) RH70 and (c) RH60 at 20 °C.

surface.[41,42] Although, it is challenging to directly observe this type of heterogeneous reaction, solution ^{1}H NMR spectroscopy was successfully used to follow the course of the reaction between the trialkoxysilanes and the LDH.

The ^{1}H solution NMR spectra of TMGPS in the presence of a dispersion of AMO-Zn_2MgAl-CO_3 LDH (acetone-d_6) are shown in Fig. 2(b) and Fig. S1.† The proton resonances at 3.53 ppm (labelled as P1) and 3.30 ppm (labelled as P2) (Fig. 2(b)) can be assigned to the (MeO)$_3$Si-protons in TMGPS and MeOH respectively. After heating the mixture at 60 °C for 3 h, the resonance at 3.30 ppm appears indicating the formation of methanol. The resonance related to methanol dramatically increased while the (MeO)$_3$Si-resonance in TMGPS decreases significantly within the first 24 h, indicating that the condensation happened quickly at 60 °C (Fig. 2b). By way of control, no change was observed when TMGPS was heated in acetone-d_6 without LDH (Fig. S2†). When TEVS was added to a dispersion of AMO-Mg_3Al-CO_3 LDH, the formation of ethanol was observed, indicating the reaction between TEVS and LDH surface hydroxyl groups has occurred (Fig. S3†). Ethanol was generated almost immediately at room temperature.

Bulk samples (2 g) of TMGPS, TEVS and TEOS modified AMO-Zn_2MgAl-CO_3 LDH were prepared in acetone at 60 °C. The XRD data indicate the basic layer structure and crystallinity of silane-modified AMO-Zn_2MgAl-CO_3 LDH remained unchanged compared to pristine AMO-Zn_2MgAl-CO_3 LDH (Fig. S4 and Table S1†). In the XRD, a small increase was observed in the c-lattice parameter from 20.4 to 21.1 and 21.7 Å for TEOS, TEVS and TMGPS treated samples respectively. The interlayer separation (6.8 Å) of pristine AMO-Zn_2MgAl-CO_3 LDH is slightly lower than that of normal carbonated containing LDH due to liberation of interlayer water molecules after thermally pre-treated at 180 °C.[43] There
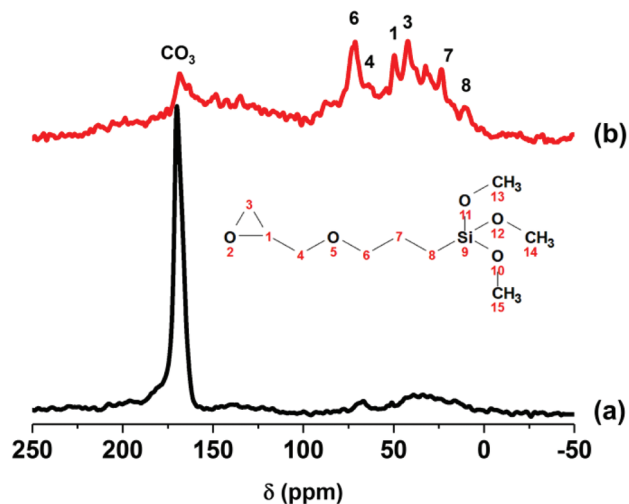

Fig. 3 ^{13}C CPMAS NMR spectra of (a) AMO-Zn_2MgAl-CO_3 LDH and (b) TMGPS modified AMO-Zn_2MgAl-CO_3 LDH.

was no change observed in the a-lattice parameter. The small expansion of the interlayer separation may result from some of silane modifying the internal surface of the LDH.

The solid-state ^{13}C CP-MAS NMR spectrum of pristine AMO-Zn_2MgAl-CO_3 LDH (Fig. 3a) exhibits one resonance at around 170 ppm, which is due to the presence of interlayer carbonate ions. After silane reaction with TMGPS, additional resonances in the range of 0–100 ppm can be observed, which correspond to the ^{13}C resonances of the 3-glycidyloxypropyl group (Fig. 3b). No resonances from the methoxy groups (marked as 13, 14, and 15 in Fig. 3) of the TMGPS can be observed, supporting the hypothesis that silane binding involves the loss of most of the methoxy groups.

The solid-state ^{27}Al NMR spectrum of the pristine AMO-Zn_2MgAl-CO_3 LDH shows a single resonance at −15 ppm, owing to the presence of octahedral Al(O_h) in the metal hydroxide structure of LDH (Fig. 4a). After silane modification, a broad, weak resonance attributed to a tetrahedral Al(T_d) environment can be observed between 20–80 ppm (Fig. 4b inset), which can be ascribed to the formation of Si–O−Al(O)$_3$ moiety on the surface of the LDH.[44,45] This resonance is broad and asymmetric, probably because the tetrahedral surface Al sites on the LDH bond to different degrees with the silane. Both TEVS and TEOS also react in a similar fashion (Fig. S5†).

The solid-state ^{29}Si CP-MAS NMR spectrum of TMGPS modified AMO-Zn_2MgAl-CO_3 LDH shows resonances between −25 and −75 ppm (Fig. S6†), which can be assigned to T^n sites of silicon (where n represents the number of Si–(O–M)$_n$ bonds formed between silane and LDH or a silicon neighbour).[30,36,46] Deconvolution of the ^{29}Si CP-MAS NMR spectrum (Table S2†) reveals that the main [29]Si resonance in TMGPS modified LDH is a monodentate T^1 site, including 1st hydrolysed monodentate at −47 ppm (49%), 2nd hydrolysed monodentate at −52 ppm (8%) and monodentate at −54 ppm (14%). In
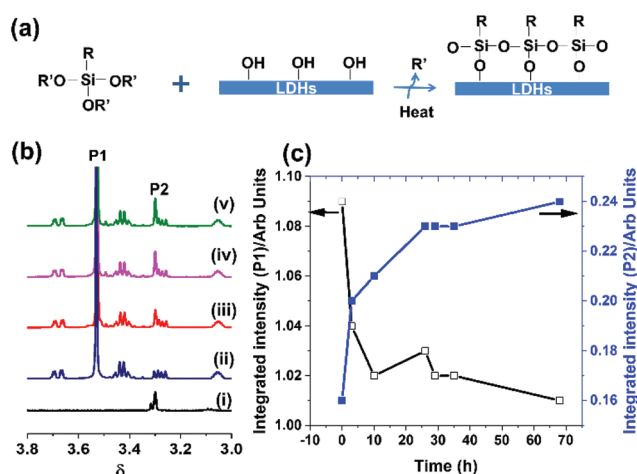

Fig. 2 (a) Proposed reaction of a trialkoxysilane with LDH surface hydroxyl groups; (b) solution ^{1}H NMR spectra of (i) methanol, (ii) TMGPS, a suspension of AMO-Zn_2MgAl-CO_3 LDH with TMGPS at 60 °C after (iii) 3 h, (iv) 33 h and (v) 68 h; (c) time dependence of the integrated intensity of the ^{1}H resonances for (MeO)$_3$Si- (P1) and MeOH (P2).
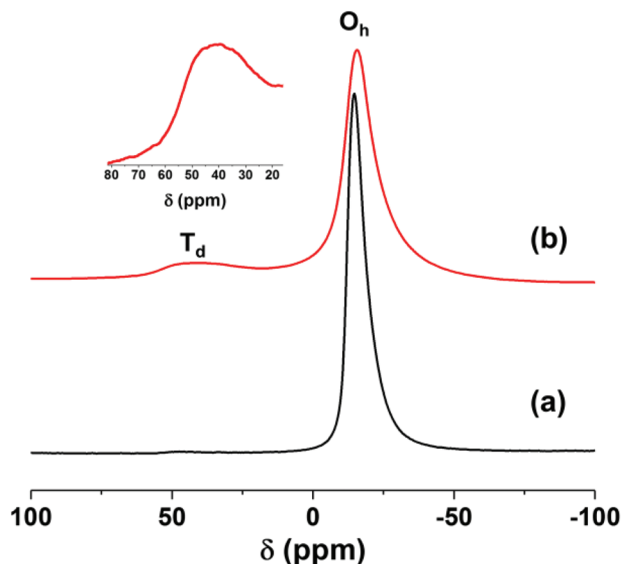
Fig. 4 ^{27}Al DP-MAS NMR spectra of (a) AMO-Zn$_2$MgAl-CO$_3$ LDH and (b) TMGPS modified AMO-Zn$_2$MgAl-CO$_3$ LDH. Inset is the enlarge range (20–80 ppm) of TMGPS modified AMO-Zn$_2$MgAl-CO$_3$ LDH at T$_d$ peak.

addition, 29% of total surface bound silicon population is due to a T^2 site, *i.e.* Si–(O–M)$_2$ involving the AMO-Zn$_2$MgAl-CO$_3$ LDH surface and/or a neighbouring silicon.

Thermogravimetric analysis (TGA) of AMO-Zn$_2$MgAl-CO$_3$ LDH and TMGPS modified AMO-Zn$_2$MgAl-CO$_3$ LDH present characteristic thermal events of an LDH (Fig. 5). The weight loss up to 200 °C is due to the release of water which includes both physiosorbed and co-intercalated interlayer water. All silane modified AMO-Zn$_2$MgAl-CO$_3$ LDHs still show some water loss at 200 °C but much less when compared with the pristine LDH (14 wt%) at 200 °C (Fig. S7, Table S3†). For example, the TMGPS modified LDH exhibits a water loss of only 4 wt% compared with that of pristine LDH (14 wt%) at
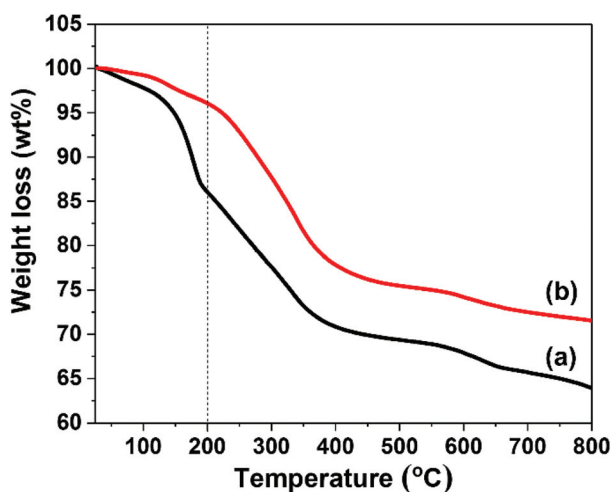
200 °C. We presume this small amount of water resides within the interlayer galleries and so was not accessible to react with the silane reagents.

The water vapour adsorption of AMO-Zn$_2$MgAl-CO$_3$ LDH and TMGPS-modified AMO-Zn$_2$MgAl-CO$_3$ LDH was evaluated at RH70 and 20 °C (Fig. 6). Pristine AMO-Zn$_2$MgAl-CO$_3$ LDH exhibits rapid water vapour adsorption, weight gain of 12 wt% compared to the dry LDH. After TMGPS surface modification, the hydrophobicity of the materials is evidenced by a significantly reduced saturation water vapour adsorption capacity (below 5 wt% after 13 days). The reduced water vapour adsorption behaviour of the other silane modified LDH are shown in Fig. S8 and Table S3.† Surface modification using vinyl silane produces a similar saturation water vapour adsorption capacity (5 wt%).

However, alkyl silane treated LDHs showed a slightly lower moisture sorption inhibition (6.5 wt% after 13 days). This could be due to a less efficient surface functionalisation by alkyl silane.

The morphology, surface area and total pore size of the AMO-Zn$_2$MgAl-CO$_3$ LDH was compared before and after surface modification. AMO-Zn$_2$MgAl-CO$_3$ LDH adopts a typical LDH platelet morphology, the as-prepared sample exhibits a particle size range of 10–250 nm (Fig. 7a). After reaction with silanes (TEVS, TEOS and TMGPS) in acetone at 60 °C, the particle size distribution remains unchanged. No significant agglomerates can be observed in the modified samples. The N$_2$ BET specific surface areas of the modified LDHs are also unaffected (Fig. S9†) while the total pore volumes are slightly larger than the pristine LDH (Fig. S10†). Silane treatment using acetone seems to be effective in achieving a high degree of surface treatment, it prevents agglomeration of the individual particles during the reaction leading to unchanged morphology, specific surface area and porosity after silane modification.
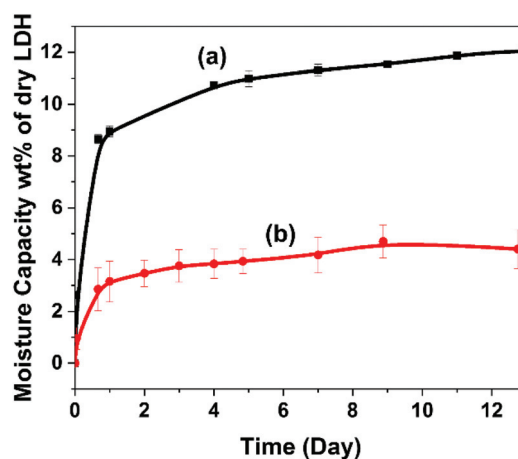

Fig. 5 TGA curves of (a) AMO-Zn$_2$MgAl-CO$_3$ LDH and (b) TMGPS modified AMO-Zn$_2$MgAl-CO$_3$ LDH.

Fig. 6 Water vapour uptake of (a) AMO-Zn$_2$MgAl-CO$_3$ LDH and (b) TMGPS modified AMO-Zn$_2$MgAl-CO$_3$ LDH in RH 70 at 20 °C.

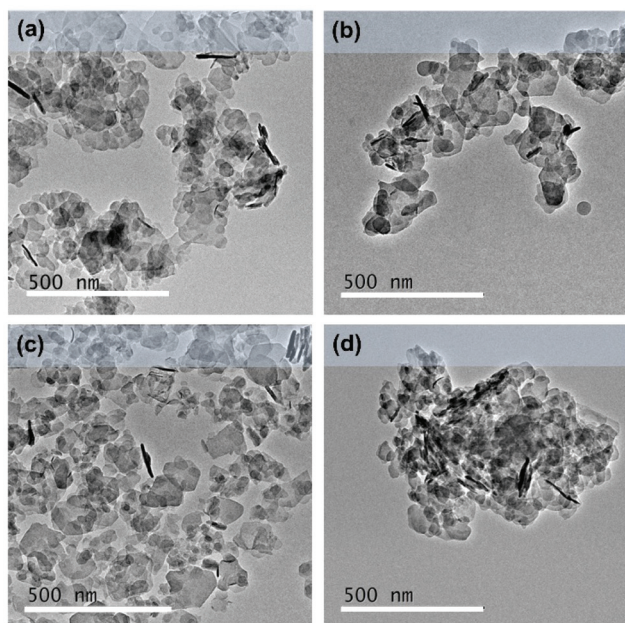**Fig. 7** TEM images of (a) AMO-Zn$_2$MgAl-CO$_3$ LDH, (b) TEVS modified AMO-Zn$_2$MgAl-CO$_3$ LDH, (c) TEOS modified AMO-Zn$_2$MgAl-CO$_3$ LDH and (d) TMGPS modified AMO-Zn$_2$MgAl-CO$_3$ LDH.

Conclusions

Trialkoxysilanes react efficiently with a dispersion of an AMO-LDH in acetone *via* elimination of the equivalent alcohol. The elimination of ethanol or methanol using either triethoxyvinylsilane (TEVS), triethoxyoctylsilane (TEOS), or (3-glycidyloxypropyl) trimethoxysilane (TMGPS) can be observed by solution ^{1}H NMR spectroscopy. Solid state ^{13}C CP-MAS, ^{27}Al DP-MAS and ^{29}Si CP-MAS NMR spectroscopy confirms the surface functionalisation.

In addition to maintaining their structure, morphology, high surface area and total pore volume, these LDHs are now more hydrophobic, displaying a saturation water vapour uptake (<4 wt%) that is *ca.* 60% lower than the untreated AMO-LDH.

Experimental

Synthesis of AMO-Zn$_2$MgAl-CO$_3$ LDH

The metal precursor solution containing 25 mmol Mg (NO$_3$)$_2$·6H$_2$O, 50 mmol Zn(NO$_3$)$_2$·6H$_2$O, 25 mmol Al (NO$_3$)$_3$·9H$_2$O and 100 mL water was added dropwise into Na$_2$CO$_3$ base solution (100 mL water with 12.5 mmol Na$_2$CO$_3$) within 1 h. The pH was kept constant around 10.0 by dropwise addition of a 4.0 M NaOH solution. After stirring for 16 h at room temperature, the mixture was filtered and washed with deionised water until pH 7. The wet LDH solid was dispersed with ethanol according to the AMOST method.[38,39] The wet LDH solid was washed with ethanol (1000 mL) by filtration and then re-dispersed in fresh ethanol (600 mL) under stirring

for 4 h. The LDH solid was then filtered and dispersed in fresh ethanol (400 mL). The final AMO-LDH solid was dried under vacuum overnight. AMO-Zn$_2$MgAl-CO$_3$ LDH has the chemical composition [Zn$_{0.47}$Mg$_{0.24}$Al$_{0.25}$(OH)$_2$](CO$_3$)$_{0.125}$·0.06(H$_2$O)·0.03 (ethanol).

Monitoring silane modification of AMO-Zn$_2$MgAl-CO$_3$ LDH

AMO-Zn$_2$MgAl-CO$_3$ LDH (20 mg) was loaded in a J. Young NMR tube followed by heating in oven at 180 °C. After 6 h, the NMR tube was closed and cooled in a desiccator under vacuum. 700 μL of a deuterated acetone (acetone-d_6) solution containing 2.8 mmol per g-LDH of the appropriate silane was introduced into the tube, then sealed and heated at 60 °C. The reaction was followed by ^{1}H NMR spectroscopy.

Bulk synthesis of silane modified AMO-Zn$_2$MgAl-CO$_3$ LDH

AMO-Zn$_2$MgAl-CO$_3$ LDH (2 g) was dried in an oven at 180 °C. After 6 h, the solid was cooled in a desiccator under vacuum followed by addition of 100 mL of acetone. Silanes (2.8 mmol per g-LDH) were introduced by slow injection under a N$_2$ flow while stirring. The slurry was refluxed at 60 °C for 18 h. The obtained solid was collected and washed with acetone. The final solid was dried in an oven at 80 °C for 18 h.

Water vapour uptake measurements

The water vapour uptake measurement was tested according to a modified Callahan's method.[47] The water vapour uptake was tested in a sealed box at room temperature (20 °C) and repeated at least three times. The relative humidity of RH99, RH70 and RH60 were generated by saturated solution of KNO$_3$, NaCl and Mg(NO$_3$)$_2$, respectively, monitored by an electrical moisture meter. Detailed measurement procedure is in shown in the ESI.†

Conflicts of interest

There are no conflicts to declare.

Acknowledgements

Notes and references

1 F. Cavani, F. Trifirò and A. Vaccari, *Catal. Today*, 1991, **11**, 173–301.
2 V. Rives, *Layered double hydroxides: present and future*, Nova Publishers, 2001.
3 D. G. Evans and R. C. Slade, in *Layered double hydroxides*, Springer, 2006, pp. 1–87.

4 C. Chen, P. Wang, T.-T. Lim, L. Liu, S. Liu and R. Xu, *J. Mater. Chem. A*, 2013, **1**, 3877–3880.

5 C. Chen, K. Y. Lee, H. Gong, Y. Zhang and R. Xu, *Nanoscale*, 2013, **5**, 4314–4320.

6 J.-M. Oh, D.-H. Park and J.-H. Choy, *Chem. Soc. Rev.*, 2011, **40**, 583–595.

7 Y. Dou, S. Xu, X. Liu, J. Han, H. Yan, M. Wei, D. G. Evans and X. Duan, *Adv. Funct. Mater.*, 2014, **24**, 514–521.

8 F. Zhang, L. Zhao, H. Chen, S. Xu, D. G. Evans and X. Duan, *Angew. Chem., Int. Ed.*, 2008, **47**, 2466–2469.

9 Y. Dou, A. Zhou, T. Pan, J. Han, M. Wei, D. G. Evans and X. Duan, *Chem. Commun.*, 2014, **50**, 7136–7138.

10 J. Yu, K. Ruengkajorn, D.-G. Crivoi, C. Chen, J.-C. Buffet and D. O'Hare, *Nat. Commun.*, 2019, **10**, 2398.

11 G. Fan, F. Li, D. G. Evans and X. Duan, *Chem. Soc. Rev.*, 2014, **43**, 7040–7066.

12 T. Baskaran, J. Christopher and A. Sakthivel, *RSC Adv.*, 2015, **5**, 98853–98875.

13 V. R. L. Constantino and T. J. Pinnavaia, *Catal. Lett.*, 1994, **23**, 361–367.

14 V. R. L. Constantino and T. J. Pinnavaia, *Inorg. Chem.*, 1995, **34**, 883–892.

15 B. Sels, D. D. Vos, M. Buntinx, F. Pierard, A. Kirsch-De Mesmaeker and P. Jacobs, *Nature*, 1999, **400**, 855–857.

16 Y. S. Gao, Q. Wang, J. Y. Wang, L. Huang, X. R. Yan, X. Zhang, Q. L. He, Z. P. Xing and Z. H. Guo, *ACS Appl. Mater. Interfaces*, 2014, **6**, 5094–5104.

17 Y. S. Gao, J. W. Wu, Q. Wang, C. A. Wilkie and D. O'Hare, *J. Mater. Chem. A*, 2014, **2**, 10996–11016.

18 Y. Z. Bao, Z. M. Huang, S. X. Li and Z. X. Weng, *Polym. Degrad. Stab.*, 2008, **93**, 448–455.

19 C. X. Zhao, Y. Liu, D. Y. Wang, D. L. Wang and Y. Z. Wang, *Polym. Degrad. Stab.*, 2008, **93**, 1323–1331.

20 X. D. Wang and Q. Zhang, *Polym. Int.*, 2004, **53**, 698–707.

21 D. G. Evans and X. Duan, *Chem. Commun.*, 2006, 485–496.

22 F. J. Labuschagne, D. M. Molefe, W. W. Focke, I. van der Westhuizen, H. C. Wright and M. D. Royeppen, *Polym. Degrad. Stab.*, 2015, **113**, 46–54.

23 A. Shimamura, E. Kanezaki, M. I. Jones and J. B. Metson, *J. Solid State Chem.*, 2012, **186**, 116–123.

24 J. Qin, P. Xie, Y. Z. Tian, H. Zhang and J. Yu, *J. Therm. Anal. Calorim.*, 2012, **110**, 1193–1198.

25 M. Badreddine, A. Legrouri, A. Barroug, A. De Roy and J. P. Besse, *Mater. Lett.*, 1999, **38**, 391–395.

26 L. Wang, S. Su, D. Chen and C. A. Wilkie, *Polym. Degrad. Stab.*, 2009, **94**, 770–781.

27 F. R. Costa, A. Leuteritz, U. Wagenknecht, D. Jehnichen, L. Häußler and G. Heinrich, *Appl. Clay Sci.*, 2008, **38**, 153–164.

28 Z. P. Xu and P. S. Braterman, *J. Mater. Chem.*, 2003, **13**, 268–273.

29 B. Wang, H. Zhang, D. G. Evans and X. Duan, *Mater. Chem. Phys.*, 2005, **92**, 190–196.

30 A. Y. Park, H. Kwon, A. J. Woo and S. J. Kim, *Adv. Mater.*, 2005, **17**, 106–109.

31 F. Wypych, A. Bail, M. Halma and S. Nakagaki, *J. Catal.*, 2005, **234**, 431–437.

32 Q. Tao, H. He, R. L. Frost, P. Yuan and J. Zhu, *Appl. Surf. Sci.*, 2009, **255**, 4334–4340.

33 Q. Tao, H. He, R. L. Frost, P. Yuan and J. Zhu, *J. Therm. Anal. Calorim.*, 2010, **101**, 153–159.

34 Q. Tao, J. Zhu, R. L. Frost, T. E. Bostrom, R. M. Wellard, J. Wei, P. Yuan and H. He, *Langmuir*, 2010, **26**, 2769–2773.

35 Q. Tao, J. Zhu, R. M. Wellard, T. E. Bostrom, R. L. Frost, P. Yuan and H. He, *J. Mater. Chem.*, 2011, **21**, 10711–10719.

36 Q. Tao, H. He, T. Li, R. L. Frost, D. Zhang and Z. He, *J. Solid State Chem.*, 2014, **213**, 176–181.

37 W. Guo, Y. Zhao, F. Zhou, X. Yan, B. Fan and R. Li, *Appl. Catal., A*, 2016, **522**, 101–108.

38 C. Chen, A. Wangriya, J.-C. Buffet and D. O'Hare, *Dalton Trans.*, 2015, **44**, 16392–16398.

39 C. Chen, M. Yang, Q. Wang, J.-C. Buffet and D. O'Hare, *J. Mater. Chem. A*, 2014, **2**, 15102–15110.

40 Q. Wang and D. O'Hare, *Chem. Commun.*, 2013, **49**, 6301–6303.

41 K. L. Mittal, *Silanes and other coupling agents*, CRC Press, 2007.

42 A. Michelot, S. Sarda, C. Audin, E. Deydier, E. Manoury, R. Poli and C. Rey, *J. Mater. Sci.*, 2015, **50**, 5746–5757.

43 V. R. L. Constantino and T. J. Pinnavaia, *Inorg. Chem.*, 1995, **34**, 883–892.

44 C. Chen, R. Felton, J.-C. Buffet and D. O'Hare, *Chem. Commun.*, 2015, **51**, 3462–3465.

45 C. Chen, C. F. Byles, J.-C. Buffet, N. H. Rees, Y. Wu and D. O'Hare, *Chem. Sci.*, 2016, **7**, 1457–1461.

46 Q. Tao, J. Zhu, R. M. Wellard, T. E. Bostrom, R. L. Frost, P. Yuan and H. He, *J. Mater. Chem.*, 2011, **21**, 10711–10719.

47 J. C. Callahan, G. W. Cleary, M. Elefant, G. Kaplan, T. Kensler and R. A. Nash, *Drug Dev. Ind. Pharm.*, 1982, **8**, 355–369.